Pergamon

Cement and Concrete Research, Vol. 27, No. 10, pp. 1591–1601, 1997

0008-8846/97 $17.00 + .00

PII S0008-8846(97)00200-7

SIMULATION OF CHLORIDE PENETRATION IN CEMENT-BASED MATERIALS

M. Masi,[1] D. Colella, G. Radaelli, and L. Bertolini
Dipartimento di Chimica Fisica Applicata, Politecnico di Milano, Piazza Leonardo da Vinci 32, I-20133 Milano, Italy

(Refereed)
(Received February 19, 1997; in final form September 26, 1997)

ABSTRACT

Corrosion of reinforcement in concrete can initiate when chloride ion concentration in contact with steel bars exceeds a threshold value. It is then of crucial importance to describe Cl^- penetration through models based on fundamental physico-chemical relationships avoiding the use of empirical parameters. Here, the multicomponent diffusional process was simulated by means of the percolation concepts. Furthermore, the adsorption of chloride within hardened cement paste was also considered. General relationships were derived to calculate binding coefficients and effective diffusivity of ions as a function of technological concrete parameters. The model explains experimental trends in a wide range of operating conditions (e.g., with and without superimposed current) both for cement paste and concrete. *© 1997 Elsevier Science Ltd*

Introduction

About 20% of reinforced concrete structures are exposed to deicing salt or to marine environment. Chloride ions, which are present in those environmental conditions, diffuse within the pores of the concrete cover up to reach reinforcing steel bars. When chloride ion concentration exceeds a certain threshold value, steel bars can depassivate also in the alkaline environment provided by concrete, leading to the onset of pitting corrosion (c.f., 1,2). Accordingly, a substantial interest in understanding the mechanism and the rate of chloride ion penetration in porous concrete exists (i.e., to design, protect, and prevent degradation of structures). Despite the economical relevance of the considered problem, the development of rigorous models for chloride ion penetration within concrete in different experimental conditions is still lacking in the literature. Most of the reported models refer to the empirical effective diffusion coefficients or neglect chloride interaction with the solid phase (3–5). Furthermore, in most of these works the model parameters where not estimated independently one from the others (6), leading to an unsuitable extrapolation to conditions different from those originally considered for the parameter fitting. Recently, some models more

[1]To whom correspondence should be addressed.

adherent to the physics of the phenomena (i.e., considering also the chloride adsorption) were presented (7–9), but still some incongruous approximations remain. For example, all the models reported in the literature consider only chloride diffusion even if the considered phenomenon is dependent on the pore solution composition (e.g., in particular by hydroxyls and cations).

The aim of this work was then to develop a mechanistic model of multicomponent ion diffusion in cement-based materials, constituted only by fundamental physico-chemical equations, to be used in different conditions and whose parameters were estimated independently one from the others. The model was developed in the framework of wetted concrete (e.g., considering all the pores filled by water), in which the ion penetration is due only to diffusion. If the concrete structures are not submerged, other phenomena can contribute to the material transport into the concrete pores, such as the capillary suction. Their influence is yet limited to the sections nearest to the surface and is negligible inside the structures. It is then possible to predict the chloride ion penetration also in these cases knowing their concentration or their total content close to the surface.

The model was developed on the basis of transient material balances for the ionic species within the cement matrix considering both the cases with and without superimposed electric current. The relevant model parameters are the effective diffusion coefficients of the species present in solution and the interaction parameters of ions with the pore structure. The former parameter was evaluated by means of percolation concepts under the framework of multicomponent diffusion. The latter parameters were estimated by measuring the adsorption isotherms of chloride ions in the cement paste. Furthermore the model parameters were correlated to the technological properties of the material (porosity, aggregates, cement content, hydration, and curing).

Modeling Aspects

The chloride ion migration in cement-based materials is the result of several phenomena: the diffusion of many ionic species in the concrete pores solution; the interactions between these ions and the concrete constituents because chlorides react with aluminates (10,11) and bind with the CSH gel (12); and finally, the hydration reactions that alter the pore structure during time (13). All these aspects were considered by the model presented here. The model was then based on conservation equations written for all the species migrating within the porous matrix (e.g., Cl^-, OH^-, and cations). The material balance considers both the diffusion ($\partial J/\partial x$) and the adsorption ($\partial \Gamma/\partial t$) processes (14,15):

$$\varepsilon \frac{\partial C_k}{\partial t} = -\frac{\partial J_k}{\partial_x} - \rho_s \frac{\partial \Gamma_k}{\partial t} \qquad k = 1, NC - 1 \tag{1}$$

where C_k, J_k, and Γ_k, are the local values of the kth species concentration, its molar flux within the porous matrix, and its adsorbed amount, respectively, whereas ρ_s and ε are the apparent density and porosity of the solid. Given concentration values were adopted as the initial and first boundary condition together with a completely developed concentration profile at the end section as the second boundary condition:

$$C_k(x, t = 0) = C_k^0(x) \tag{2}$$

$$C_k\,(x = 0,\, t) = C_k^{sup}\,(t) \tag{3a}$$

$$\left.\frac{\partial C_k}{\partial x}\right|_{x=L} = 0 \tag{3b}$$

It is important to note that the first boundary condition is a function of time to consider the possibility of transient external conditions for the wetting solution. In a solution containing NC ions, the independent species are only $NC - 1$ due to the electroneutrality constraint (15):

$$\sum_{m=1}^{NC} z_m C_m = 0 \tag{4}$$

The molar flux of one species was then evaluated as follows (15):

$$J_k = -\sum_{m=1}^{NC-1} D_{k,m}^{eff} \frac{\partial C_m}{\partial x} - u_k^{eff} C_k F \frac{\partial \varphi}{\partial x} \tag{5}$$

where $D_{k,m}^{eff}$, u_k^{eff}, F and φ are the effective diffusion coefficient of the kth ion due to the mth concentration gradient, the effective mobility of the kth ion, the Faraday constant, and the local electric potential value, respectively. Stefan-Maxwell equations were adopted to describe multicomponent diffusion within the concrete matrix because in an ionic multicomponent system the diffusion of one species is influenced by all the others (16). The use of Eq. 5 is one of the qualifying points of the model presented here, being the only rigorous way to describe multicomponent diffusion. The effective diffusion coefficients were estimated from the molecular ones through the percolation theory as described in (17,18), whereas the molecular diffusion coefficients $D_{k,m}$ were evaluated using the irreversible thermodynamics as described in (19). Those important points will be addressed in detail below.

When an electrical current is superimposed, such as in the cases of cathodic protection and prevention, the chloride penetration can be inhibited by the electrostatic field and the migration of each ion depends also on its mobility within the field. The mobility coefficients were related to the diffusion coefficients by the Nernst-Planck theory ($u_k^{eff} = D_{k,k}^{eff}/RT$) (15,16,20,21). Obviously, when an electrical current is superimposed the net charge flux has to be proportional to the superimposed current density i:

$$\sum_{i=1}^{NC} z_i J_i = \frac{i}{F} \tag{6}$$

where z_i is the ionic valence. As a consequence of the rigorous evaluation of the diffusion coefficients matrix, the following equation is always satisfied (19):

$$\sum_{i=1}^{NC}\left(\sum_{j=1}^{NC} z_i D_{i,j}^{eff} \frac{\partial C_j}{\partial x}\right) = 0 \tag{7}$$

and then the electrostatic potential gradient can be calculated from Eqs. 5–7 leading to the following relationship where the electrostatic potential φ is related to the ionic concentrations and to the diffusion coefficients:

$$\frac{F}{RT}\frac{\partial \varphi}{\partial x} = i\left(F \cdot \sum_{k=1}^{NC} z_k^2 D_{k,k}^{eff} C_k\right)^{-1} \tag{8}$$

Chloride adsorption within the cement matrix ($\partial\Gamma/\partial t$) in Eq. 1 was described by means of a Langmuir isotherm (6–9) whose parameters were fitted on experimental adsorption data. Those parameters were estimated using the procedure described in (7) to evaluate the adsorption effects independently from the diffusion processes. The adsorption of all the ions present in pore solution, except Cl^-, was neglected. In order to keep the electroneutrality constraint, the binding of chloride ions was balanced by the dissolution of hydroxyl ions from the solid phase (8,22):

$$\frac{\partial \Gamma_{Cl}}{\partial t} = -\frac{\partial \Gamma_{OH}}{\partial t} \tag{9}$$

The hydration reactions affect the concrete capillary porosity because the hydration products occupy a volume about twice that of the silicates and aluminates. The main consequence is that the chloride penetration rate decreases until the porosity reaches a threshold value. After that point, the diffusion rate is about constant because it takes place in the gel pores (23).

The hydration degree (i.e., the fraction of silicates reacted) was evaluated by the relationships reported in (24) describing calcium silicates (e.g., C_2S and C_3S) conversions into their hydrated products. An approximation of the hydration degree α can be obtained from an average of the conversions as reported below:

$$\alpha = 1 - 0.5\cdot[(1 + 1.67\tau)^{-0.6} + (1 + 0.29\tau)^{-0.48}] \tag{10}$$

where τ is the time passed since the hydration started. Also, the system porosity depends on the hydration degree, being its value calculated through the following relationship (13):

$$\varepsilon_{cp}(\alpha) = (w/c - 0.36\alpha)\cdot\rho_{cp} \tag{11}$$

where ρ_{cp} and w/c are the cement paste density and the water/cement ratio, respectively. The concrete porosity, neglecting aggregates porosity, can be calculated by the following relationship:

$$\varepsilon_c(\alpha) = \varepsilon_{cp}\cdot(3.175\cdot10^{-4} + w/c\cdot10^{-3})\cdot P_c \tag{12}$$

where ε_{cp} and P_c are the porosity of the cement paste within the concrete and the cement content (kg of cement/m^3 of concrete), respectively. The cement paste density was obtained by a weighted average between cement and water densities:

$$\rho_{cp} = \frac{1 + w/c}{(0.3175 + w/c)}\cdot1000 \tag{13}$$

Finally, the concrete density was obtained directly from its cement content (P_c):

$$\rho_c = P_c\cdot(1 + w/c + a/c) \tag{14}$$

where a/c is the aggregates/cement ratio.

The partial differential equation system (Eqs. 1, 5, and 8) was solved numerically using the finite differences method for the spatial dimension and a 4th order Runge-Kutta method for the time integration (25). In summary, the important model parameters are the diffusion coefficients and the adsorption isotherm parameters. Their estimation is addressed in detail in the following sections.

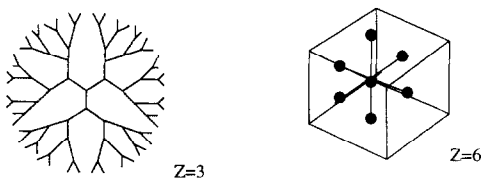

FIG. 1.
Schematic of a bidimensional Bethe lattice (coordination number $Z = 3$) and tridimensional one (coordination number $Z = 6$)

Diffusion Coefficients

Initially, molecular diffusion coefficients were calculated using irreversible thermodynamics (19) applied to a multicomponent ionic system. Given NC ionic species, the result of the calculation is a $(NC - 1) \times (NC - 1)$ matrix of diffusion coefficients. Considering that the molecular diffusion coefficients $d_{k,m}$ are not influenced by electrostatic field, the NCth value (due to the NCth concentration gradient) can be obtained imposing the electroneutrality constraint in the form of Eq. 7 to the same system with no superimposed current, being $D_{NC,j} = 0$ for $j \neq NC$. As described in (19), the values of the molecular diffusion coefficients were calculated as a function of solution concentration.

The effective diffusion coefficients were then calculated from the molecular ones in the framework of the percolation theory (17), where the topology of the solid was described using a network representation of the pore space, called Bethe lattice. This network is characterized by a coordination number Z that represents the number of bonds connected to a given site of the network. The coordination number Z fully describes the transport properties within the lattice. An example of Bethe network is skectched in Figure 1. Porous structures are usually represented by Z ranging in the interval 4–12, with $Z = 6$ and $Z = 12$ correspondent to the cubic and to the Voronoi lattices, respectively (18).

Accordingly to percolation theory, long-distance transport is possible only if the system porosity exceeds a threshold value related to the coordination number ($\varepsilon_{th} = 1/z - 1$) (26). In the case where $\varepsilon_{pc} > \varepsilon_{th}$, diffusion almost exclusively occurs in capillary pores and the effective diffusion coefficients can be calculated as follows (18):

$$D_{k,m}^{eff} = D_{k,m} \cdot \frac{Z - 1}{Z - 2} (\varepsilon_{pc} - \varepsilon_{th}) \tag{15}$$

When system porosity decay below the percolation threshold ($\varepsilon_{pc} < \varepsilon_{th}$), transport takes place in gel pores and the effective diffusion coefficients can be calculated as follows (23):

$$D_{k,m}^{eff} = (0.001 \div 0.004) D_{k,m} \tag{16}$$

When the diffusion in concrete is examined, a continuous path along the slab due to the interfacial zone around aggregates can be always found (27). Therefore, in such a case, the percolation threshold cannot be reached and effective diffusion coefficients are always calculated by Eq. 15.

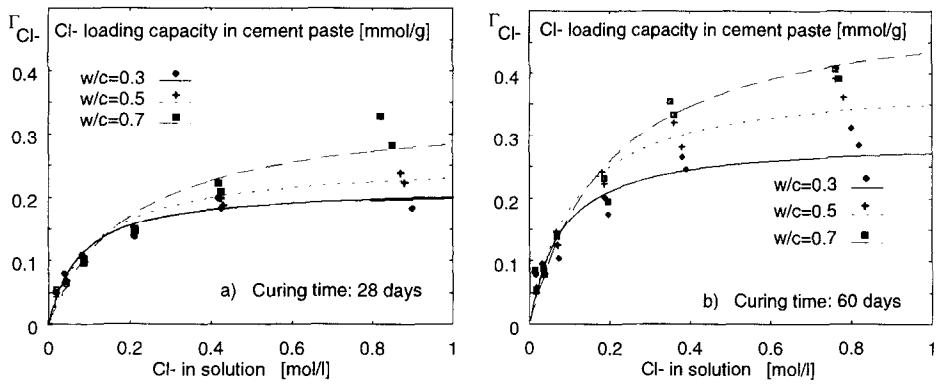

FIG. 2.

Chloride adsorptivity in Portland I cement paste as a function of their concentration in solution. Experimental data and Langmuir fitting. Isotherms measured at room temperature for different curing time and w/c ratio.

Chloride Adsorption

As already pointed out, chloride ions strongly interact with the hardened cement constituents. Here, such complex phenomena were assimilated to an adsorption over the solid matrix, whose behavior can be described by a Langmuir-type adsorption isotherm (6–9,28):

$$\Gamma_{Cl^-} = \frac{k\Gamma^{\infty} C_{Cl^-}}{1 + kC_{Cl^-}} \tag{17}$$

where C (mol/L) and Γ (mmol/g) are the liquid and solid-phase concentrations of chloride ions. The isotherm parameters k and Γ^{∞} were obtained from adsorption experiments here performed with a Portland CEM I 42.5 cement. Particularly, cement pastes with different water/cement ratios (i.e., w/c = 0.3, 0.5, and 0.7) and curing times (28 and 60 days) were grounded to a fine powder (diameter <0.18 mm). A measured amount of these powders was then immersed into NaCl solutions with different concentrations (i.e., 0.02, 0.05, 0.1, 0.25, 0.5, and 1 mol/L). Two different cases were considered. The former deals with cement pastes cured for 28 days, whereas the latter deals with pastes cured for 60 days. Besides the experimental verification that the system transitory ends within 4 h after the immersion, the 28 days cured pastes were submerged for 12 h while those cured for 60 days were submerged for another 60 days in order to reach the complete hydration. Liquid-phase concentrations were measured by titration with a Cl^--ion-sensitive electrode and the Cl^- amount in the solid-phase was determined by the difference between the initial and final solution concentrations. The evaporable water content was measured for all the cement pastes used, and, finally, the Cl^- amount in the solid phase was expressed as a function of the dry weight of cement paste in the measuring unit. All the experiments above were performed at room temperature.

The aim was to evaluate the effects of hydration and water/cement ratio on the chloride adsorption independently from the estimation of the diffusion parameters. An example of the measured adsorption isotherms is illustrated in Figure 2, where the effect of hydration degree

TABLE 1
Summary of Porosity and Coordination Number Values Used in Simulations

Cement based material	ε (30 days)	ε (α = 1)	Z	min D_{eff}/D_m	max
submerged cement pastes (w/c = 0.5)	0.4	0.28	3.8–4	0.004	0.06
submerged cement pastes (w/c = 0.7)	0.65	0.5	3–3.2	0.004	0.2
submerged concrete	0.09–0.13	0.09–0.13	9–11	0.004	0.02
concrete in air	0.09–0.13	0.09–0.13	9–11	0.001	0.02

and water/cement ratio is reported. An increase of the chloride adsorption with the considered parameters can be clearly observed.

General relationships for adsorption parameters were then obtained by fitting the experimental data by regression:

$$\begin{cases}\Gamma_{cp}^{\infty}(\tau, w/c) = 0.145 + [\alpha(\tau) - 0.5]\cdot(w/c + 0.01) \\ k_{cp}(w/c) = 19 - 20\cdot w/c\end{cases} \quad \text{with} \quad \begin{matrix}\tau > 28 \text{ days} \\ 0.3 \le w/c \le 0.7\end{matrix} \tag{18}$$

The above parameters, obtained for cement pastes, can be generalized to concretes assuming that aggregates do not contribute to chlorides adsorption:

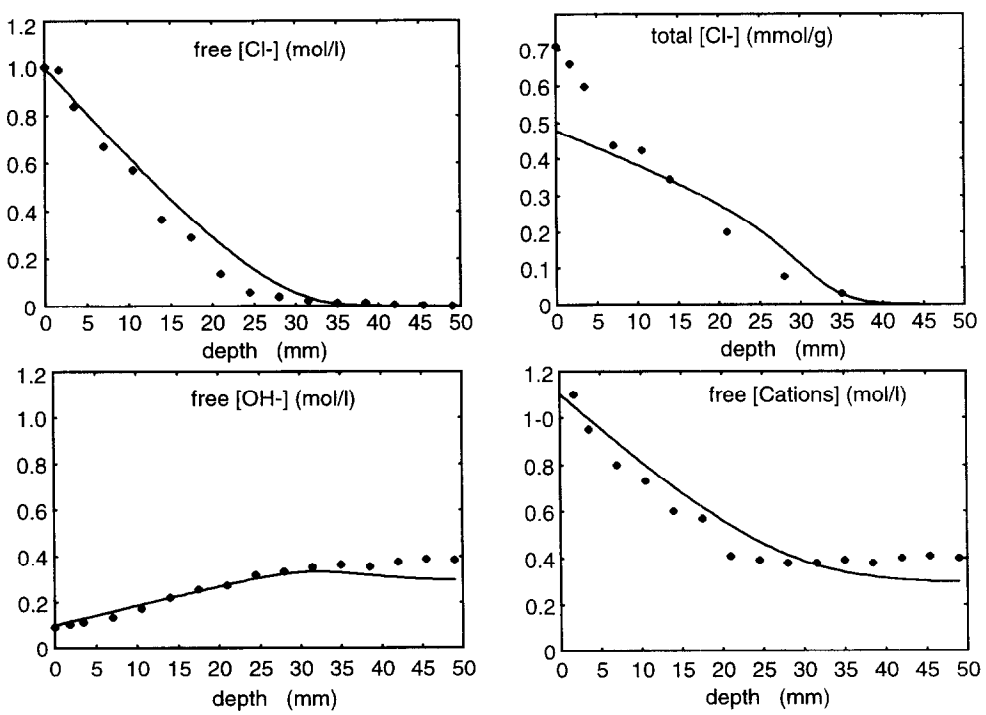

FIG. 3.
Comparison between calculations and experimental data of ref. (8). Cl^-, OH^-, and cations concentration vs. depth.

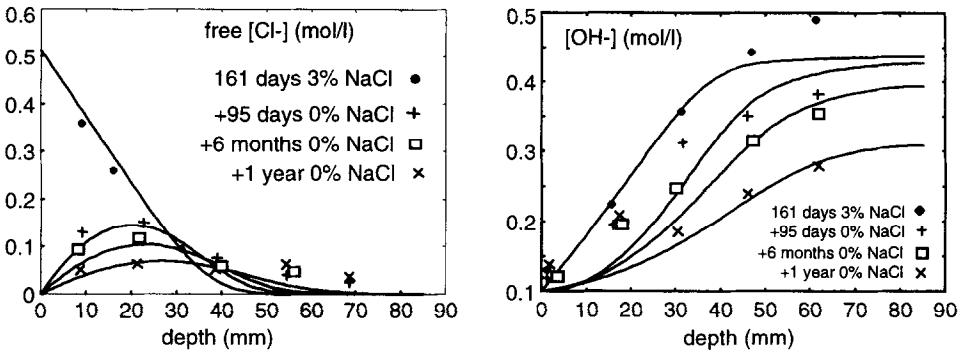

FIG. 4.
Comparison between the calculated and the experimental free Cl^- and OH^- concentrations vs. depth and time in condition of ref. (29).

$$\begin{cases} \Gamma_c^{\infty} = \Gamma_{cp}^{\infty} \cdot \dfrac{1 + w/c}{1 + w/c + a/c} \\ K_c = k_{cp} \end{cases} \tag{19}$$

Results and Discussion

Many simulations were performed to test the model reliability in predicting chloride penetration in hardened cement pastes and concretes as a function of time. The basic idea was to simulate as many as possible experimental trends without the use of adjustable parameters on the particular experimental conditions considered in each simulation. All the simulations reported below were performed considering a ternary system constituted by Na^+, Cl^-, and OH^-. The role of different cations than Na^+ was also tested, showing an almost negligible difference in behavior with respect to the basic case. Moreover, cations are less mobile than OH^- in the systems here examined, OH^- being the ion in charge to keep the solution

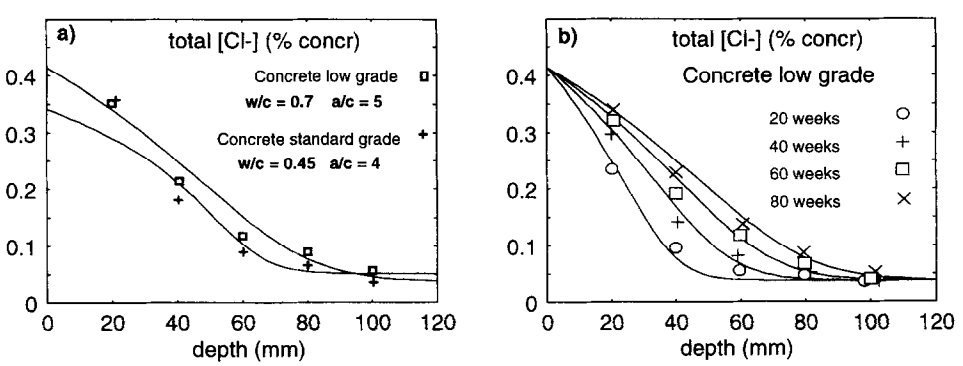

FIG. 5.
Comparison between the calculated and the experimental total Cl^- content vs. depth and time in condition of ref. (30): *a*) low grade and standard grade concrete (80 weeks); *b*) low grade concrete at four different times.

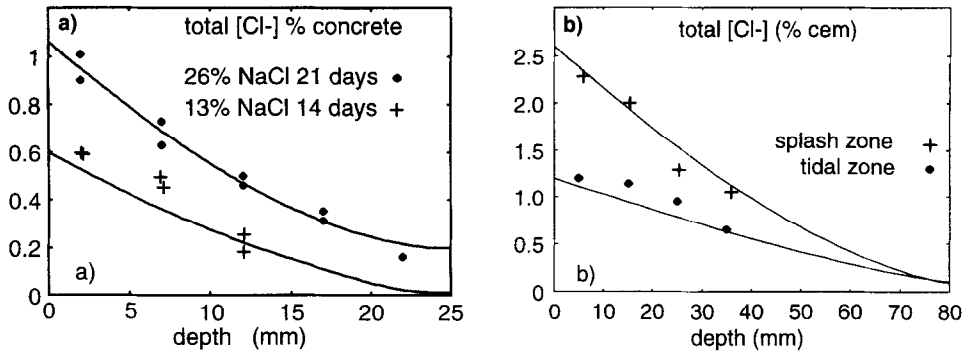

FIG. 6.
Comparison between the calculated and the experimental total Cl^- content vs. depth: *a*) condition of ref. (7); *b*) condition of ref. (5), concrete exposed to splash and tide.

electroneutrality due to its larger diffusivity value. For all the simulations, the coordination number Z of the Bethe lattice was estimated from the porosity value. The former value was estimated about 4 for cement pastes and about 10 for concretes, whereas the latter was ranging about 0.5 for cement pastes and about 0.10 for concretes as summarized in Table 1.

One of the most comprehensive sets of experimental data was reported in (8) where free and total chloride, free OH^-, and cations concentrations were measured as a function of depth for a 28-days cured cement paste ($w/c = 0.5$) submerged for 100 days in 1M NaCl solution. The comparison between the calculated values and the experimental ones is illustrated in Figure 3. A good agreement between simulation and experiments is evidenced considering that no adjustment of the model parameter was performed.

Another interesting case is that reported in (29) where a 28-days cured cement paste was initially submerged in a 3% NaCl solution for 161 days and then in pure water for 365 days. Also in this case, illustrated in Figure 4, satisfactory agreement between the calculated and the experimental data can be observed.

Considering concretes instead of cement pastes, two different types of concrete were

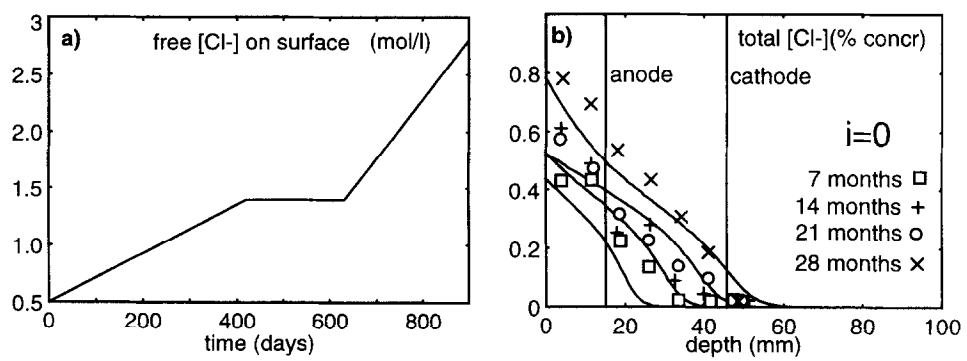

FIG. 7.
Comparison between calculations and experiments of ref. (31); *a*) external Cl^- concentration vs. time (estimated value); *b*) total Cl^- content vs. depth and time, case without superimposed electric current.

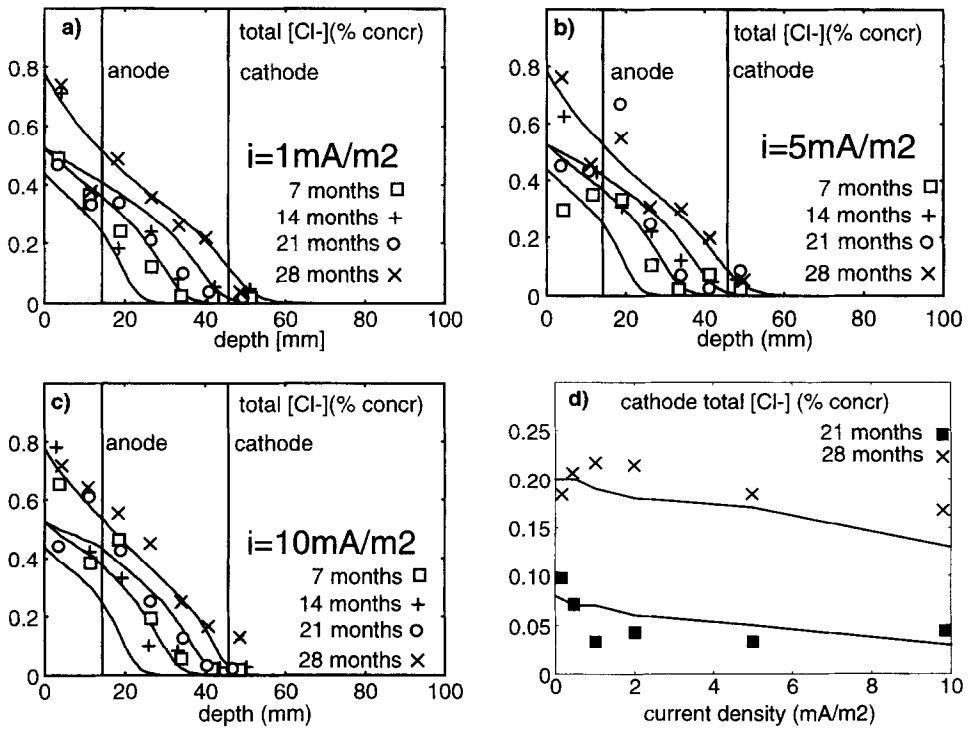

FIG. 8.

Comparison between calculations and experiments of ref. (31): *a*), *b*), *c*) cases with 1, 5, and 10 mA/m2 current density, respectively; *d*) total Cl^- content at cathode vs. current density.

examined in (30). Also in this case, the simulations illustrated in Figure 5 show a good agreement with the experimental data. Similar experiments are illustrated in Figure 6a, where the experimental conditions reported in (7) were simulated. Also, transient boundary conditions were examined simulating the experiments reported in (5), where concrete exposed to both tide and splashes was studied inside a spray chamber. The transient boundary conditions were here obtained interpolating the experimental values reported in the quoted reference. The comparison between experiments and calculation for the considered example is shown in Figure 6b.

The effect of current flowing in the concrete cover was studied with regard to the cathodic prevention conditions and were examined by simulating the experiments reported in (31), where the penetration of chloride as a function of time and of depth was measured for different applied current density values. The concrete was subjected to drying/wetting cycles with a NaCl solution. The superficial content of chloride ions changed during time due to evaporation and wetting cycles as illustrated in Figure 7a. As shown in Figure 8, the electric current inhibits the chloride ion penetration within the concrete with respect to the case without superimposed current density illustrated in Figure 7b.

Concluding Remarks

The simulations reported above demonstrate that the chloride ion penetration in cement pastes and concretes can be predicted "a priori" if the proper parameters are correctly

estimated. In particular, various types of concretes can be studied, because the only properties needed for the simulations can be easily measured: the adsorption parameters and the system porosity. The model proposed can be useful for the estimation of the service life of reinforced concrete structures after the beginning of the design procedure, avoiding costly on site experimentation.

References

1. P. Pedeferri and L. Bertolini, La Corrosione nel Calcestruzzo e negli Ambienti Naturali, McGraw-Hill, Milano, 1996.
2. S. Chatterji, Il Cemento 19, 139 (1995).
3. P.S. Mangat and K. Gurusami, Cem. Concr. Res. 17, 385 (1987).
4. H. Lin, Corrosion 46, 964 (1990).
5. P.S. Mangat and B.T. Molloy, Mag. Concr. Res. 46, 279 (1994).
6. S. Diamond, Cem. Concr. Aggr. 8, 97 (1986).
7. C.J. Pereira and L.L. Hegedus, Int. Chem. Eng. Symp. Ser. 87, 427 (1984).
8. G. Sergi, S.W. Yu and C.L. Page, Mag. Concr. Res. 44, 63 (1992).
9. V.G. Papadakis, M.N. Fardis and C.G. Vayenas, Chem. Eng. Sci. 51, 505 (1996).
10. P. Lambert, C.L. Page and N.R. Short, Cem. Concr. Res. 15, 675 (1985).
11. Rasheeduzzafar, S. Ehtesham Hussain and S.S. Al-Saadoun, Cem. Concr. Res. 21, 777 (1991).
12. J.J. Beaudoin, V.S. Ramachandran and R.F. Feldman, Cem. Concr. Res. 20, 875 (1990).
13. M. Collepardi, Scienza e Tecnologia del Calcestruzzo, Hoepli, Milano, 1991.
14. E. Santacesaria, M. Morbidelli, P. Danise, M. Mercenari and S. Carrà, Ind. Eng. Chem. Proc. Des. Dev. 21, 440 (1982).
15. J. Newman, Electrochemical Systems, Chemical and Catalytic Reaction Engineering, J.J. Carberry and A. Varma (eds), M. Dekker, New York, 1987.
16. R.B. Bird, W.E. Stewart and E.N. Lightfoot, Transport Phenomena, J. Wiley, New York, 1960.
17. S. Reyes and K.F. Jensen, Chem. Eng. Sci. 40, 1723 (1985).
18. P. Corrente and M. Masi, Proceedings of 1st Conf. Chemical and Process Engineering, AIDIC 337 (1993).
19. R.P. Wendt, J. Phys. Chem. 69, 1227 (1965).
20. G. Bianchi and T. Mussini, Elettrochimica, Tamburini Masson, Milano, 1976.
21. C. Andrade, M.A. Sanjuan and C. Alonso, NACE Int. Corrosion/93 Conference, NACE, Houston, Paper 319.
22. E.M. Theissing, P.V. Hest-Wardenier and G. de Wind, Cem. Concr. Res. 8, 683 (1978).
23. D.P. Bentz and E.J. Garboczi, J. Mat. Sci. 27, 2083 (1992).
24. V.G. Papadakis, C.G. Vayenas and M.N. Fardis, AIChE J. 35, 1639 (1996).
25. B. Carnhan, H.A. Luters and J.O. Wilkes, Applied Numerical Methods, J. Wiley, New York, NY (1969).
26. B. Fisher and F. Essam, J. Math. Phys. 2, 609 (1961).
27. D. Winslow, M.D. Cohen, D.P. Bentz, K.A. Snyder and E.J. Garboczi, Cem. Concr. Res. 24, 25 (1994).
28. D.M. Ruthven, Principles of Adsorption and Adsorption Processes, J. Wiley, New York, NY (1984).
29. J. Tritthart, Cem. Concr. Res. 22, 129 (1992).
30. S.K. Roy, K.C. Liam and D.O. Northwood, Cem. Concr. Res. 23, 1289 (1993).
31. L. Bertolini, F. Bolzoni, P. Pedeferri and T. Pastore, NACE Int. Corrosion/97 Conference, NACE, Houston, Paper 97244 (in press).